JOURNAL OF Materials CHEMISTRY

Nanosized hydroxyapatite powders from microemulsions and emulsions stabilized by a biodegradable surfactant

G. K. Lim,[a] J. Wang,*[a] S. C. Ng[b] and L. M. Gan[c]

[a]*Department of Materials Science,* [b]*Department of Physics,* [c]*Department of Chemistry, The National University of Singapore, Singapore 119260. E-mail: maswangj@nus.edu.sg*

Received 10th December 1998, Accepted 7th May 1999

Ultrafine hydroxyapatite powders have been successfully synthesized in inverse microemulsions and emulsions consisting of petroleum ether as the oil phase, 1.0 M $CaCl_2$ solution as the aqueous phase and biodegradable KB6ZA as the surfactant. The titration of 0.6 M $(NH_4)_2HPO_4$ aqueous solution into the inverse microemulsion and emulsions containing 25.0 and 35.0 wt% aqueous phase, resulted in hydroxyapatite precursors that were nanometer sized and more or less spherical in morphology. However, they underwent a considerable degree of particle coarsening when calcined at 650 °C for 6 h. A nanocrystalline hydroxyapatite powder, which exhibited a dendritic agglomerate morphology, was synthesized in an oil-in-water emulsion containing 90.0 wt% aqueous phase. It shows an average particle size of 25 nm upon calcination at 650 °C for 6 h, as little particle coarsening and growth in crystallite size were observed at the calcination temperature. The inverse microemulsion- and emulsion-derived hydroxyapatites exhibit a degree of type B carbonate substitution, which cannot be eliminated by calcination in air at 650 °C.

Introduction

Synthetic hydroxyapatite (HA) is a well-known biocompatible and bioactive material that has been widely used in many clinical applications.[1–3] It is commonly employed as a coating for bioinert metallic and ceramic substrates, such as titanium and alumina,[4,5] for use as implants. Hydroxyapatite also shows a high capacity for ion exchange with heavy metal ions owing to its unique crystal structure and composition.[6] Thus, it has been investigated as a filter for removing heavy metals from aqueous solutions.[7] There are many other applications of hydroxyapatite, including: high performance liquid chromatography (HPLC) for the separation of proteins and nuclec acids due to its ability to interact electrostatically with these molecules; gas sensing; and catalysis.[8]

Nanosized hydroxyapatite particles have been successfully synthesized from microemulsions.[9,10] They possess improved powder characteristics that make them superior in many of the above mentioned applications. The microemulsion-derived hydroxyapatite powders exhibit a high specific surface area, lowered degree of particle agglomeration and narrowed particle size distribution. However, these previous studies employed poly(oxyethylene) nonylphenol ethers (NP5 and NP9) as the surfactants, which belong to the generic group of alkylphenol ethoxylates, and there is a big doubt over their biodegradability.[11–13] In contrast, the nonionic surfactants belonging to the generic group of alcohol ethoxylates are completely hydrolysable and therefore they exhibit excellent biodegradability.[12]

As the suitability of poly(oxyethylene) nonylphenol ethers (*e.g.* NP5 and NP9) for use as nonionic surfactants on a large scale is in doubt as a result of their low biodegradability, it is both scientifically interesting and technologically challenging to study the feasibility of using a biodegradable surfactant for synthesizing nanophase materials in water-in-oil microemulsions, water-in-oil emulsions, and in particular, oil-in-water emulsions which only require small amounts of the oil and surfactant phases. The objectives of this paper are two-fold: (i) to investigate whether ultrafine hydroxyapatite particles can be synthesized in inverse water-in-oil microemulsions and emulsions using a biodegradable alcohol ethoxylate as the surfactant; and (ii) to study whether a nanocrystalline HA powder can be synthesized in an oil-in-water emulsion, which will offer the advantage of using only small amounts of the oil and surfactant phases.

Experimental procedure

The chemicals used as the starting materials included: (i) 1.0 M $CaCl_2$ aqueous solution; (ii) 0.6 M $(NH_4)_2HPO_4$ aqueous solution (both from Merck Co., USA); (iii) petroleum ether (PE) of boiling point 120–160 °C (BDH, UK); (iv) Empilan KB6ZA, which is a lauryl alcohol condensed with 6 mol equiv. of ethylene oxide (Albright and Wilson Asia Ptd Ltd, Singapore); and (v) distilled ethanol.

By following the procedure as detailed in Ref. 10, the phase diagrams for the ternary system consisting of 1.0 M $CaCl_2$ solution as the aqueous phase, PE as the oil phase and KB6ZA as the surfactant at 25 and 34.5 °C, were established. Three compositions were then chosen for the preparation of hydroxyapatite precursors at 34.5 °C: (i) a transparent microemulsion consisting of 25.0 wt% 1.0 M $CaCl_2$ aqueous phase, 52.5 wt% PE and 22.5 wt% KB6ZA; (ii) a translucent composition consisting of 35.0 wt% 1.0 M $CaCl_2$ aqueous solution, 45.5 wt% PE and 19.5 wt% KB6ZA; and (iii) a turbid emulsion composition consisting of 90.0 wt% 1.0 M $CaCl_2$ aqueous solution, 7.0 wt% PE and 3.0 wt% KB6ZA. The procedures for the syntheses of hydroxyapatites in microemulsion and emulsions are detailed in Ref. 10. Hydroxyapatite powders obtained from the three compositions above were characterised for particle size and morphology using BET specific surface area analysis (Quantachrome NOVA2000) and TEM (JEOL-100CX). Their phase purity was measured using XRD phase analysis (Cu-Kα, Philips Model PW1729), FTIR (BIORAD) and X-ray photoelectron spectroscopy (VG ESCALAB MkII).

Results and discussion

The partial phase diagrams at 25 and 34.5 °C, for the ternary system consisting of 1.0 M $CaCl_2$ aqueous solution as the water phase, PE as the oil phase and KB6ZA as the surfactant are shown in Fig. 1. The shaded regions represent transparent microemulsion compositions. At 25 °C the ternary mixtures are considerably viscous and gel-like. However, at 34.5 °C they are fluid-like and optically transparent for all the compositions

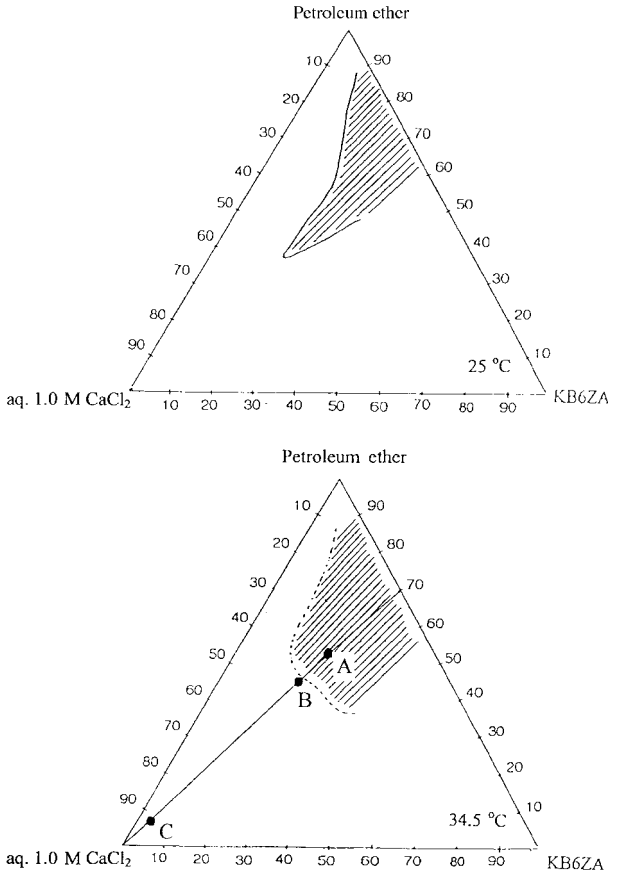

Fig. 1 Partial phase diagrams established for the ternary system consisting of 1.0 M $CaCl_2$, KB6ZA and PE at 25 and 34.5 °C.

in the shaded region. KB6ZA exhibits a cloud point temperature of 36 °C, above which it undergoes dehydration and below which the degree of hydrogen bonding between the ethylene oxide groups and water molecules becomes extensive.[14] Therefore, high viscosity was observed at room temperature because KB6ZA undergoes an extensive degree of hydration. At 34.5 °C, which is near the cloud point, the hydrogen bonds are disrupted, such that the flexibility of surfactant molecules at the oil and water interface is enhanced. Thus the ternary compositions exhibit a low viscosity and fluid-like behaviour. As indicated in the partial phase diagram at 34.5 °C, the compositions marked A (transparent), B (translucent) and C (turbid) containing 25.0, 35.0 and 90.0 wt% of 1.0 M $CaCl_2$ aqueous phase, respectively, were chosen for the preparation of hydroxyapatites.

Fig. 2 shows the electrical conductivity as a function of 1.0 M $CaCl_2$ content for the compositions containing oil and surfactant at a fixed weight ratio of 7:3 at 34.5 °C. The electrical conductivity is very low throughout the composition region 0.0–80.0 wt% 1.0 M $CaCl_2$, although there is a slight increase in conductivity as the aqueous content increases. This indicates that the transparent compositions containing <34 wt% aqueous phase are inverse microemulsions, where the conducting aqueous phase is confined as dispersed droplets in the oil phase. The bicontinuous microemulsion, which exhibits a high electrical conductivity due to the occurrence of interconnecting aqueous channels, does not exist in this system. This is therefore considerably different from the ternary system containing NP5 or NP9 as the nonionic surfactant and cyclohexane as the oil phase.[10] The sudden increase in electrical conductivity at >80 wt% aqueous phase is due to the latter becoming a continuous phase by forming turbid normal emulsions. Thus, the chosen compositions A and C are believed to be a transparent water-in-oil (inverse) microemulsion and a turbid oil-in-water emulsion, respectively. The translucent composition B, which is close to the microemulsion/emulsion boundary, is an inverse emulsion as indicated by its low conductivity.

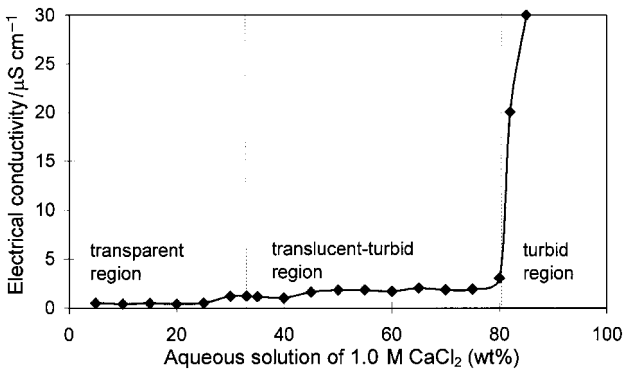

Fig. 2 Electrical conductivity at 34.5 °C as a function of content of aqueous 1.0 M $CaCl_2$ for compositions containing oil and surfactant at a fixed weight ratio of 7:3.

Fig. 3(a–c) are TEM micrographs showing the HA precursors obtained from compositions A, B and C, respectively. The powders obtained from compositions A and B consist of spherical particles that are well dispersed, coupled with a rather uniform particle size distribution. The spherical particle morphology is an indirect indication that the precipitation reaction between $CaCl_2$ and $(NH_4)_2HPO_4$ took place within the dispersed aqueous droplets. The HA particles obtained from composition A are apparently smaller than those from composition B due to a higher aqueous content in the latter. The reaction of $CaCl_2$ and $(NH_4)_2HPO_4$ in a larger aqueous domain invariably leads to the formation of larger HA particles. The HA particles obtained from composition C, which is an oil-in-water emulsion, are nanosized and are aligned as dendritic agglomerates, which is a result of the fact that the precipitation reaction took place in a continuous aqueous phase. Such a dendritic morphology is commonly observed for HA particles obtained by conventional precipitation from an aqueous phase.

Fig. 4(a–c) show TEM micrographs for the hydroxyapatite powders obtained from compositions A, B and C, respectively, and calcined at 650 °C for 6 h. The powder obtained from composition A consists of particles of 40–50 nm, which are rounded in morphology. It has undergone a high degree of particle coarsening compared to the nanoparticles before calcination, shown in Fig. 3(a). The hydroxyapatite powder obtained from composition B exhibits an apparently larger particle size (80–100 nm), although the particle morphology is similar to that of the powder obtained from composition A. This may easily be accounted for by the fact that the particle size of the latter was larger in the precursor state than that of the former prior to calcination at 650 °C for 6 h, as demonstrated in Fig. 3(a,b). In a remarkable contrast, the hydroxyapatite powder obtained from composition C retained its nanosized features, together with the dendritic agglomerates. It underwent little coarsening in particle size at the calcination temperature and the dendritic morphology was preserved.

In order to confirm what was observed using TEM, the powders obtained from the three compositions were characterised for their specific surface areas. Specific surface areas of 43.9, 13.5 and 74.6 $m^2\ g^{-1}$ were measured for the HA powders from the inverse microemulsion (composition A), inverse emulsion (composition B) and oil-in-water emulsion (composition C), after they had been calcined at 650 °C for 6 h. On the basis of these, average particle sizes of 43, 140 and 25 nm were estimated for the three powders, respectively. Calcination at 650 °C resulted in a much larger degree of particle coarsening of hydroxyapatite crystallites in the former two than that in the powder obtained from the oil-in-water emulsion containing 90.0 wt% 1.0 M $CaCl_2$ aqueous phase.

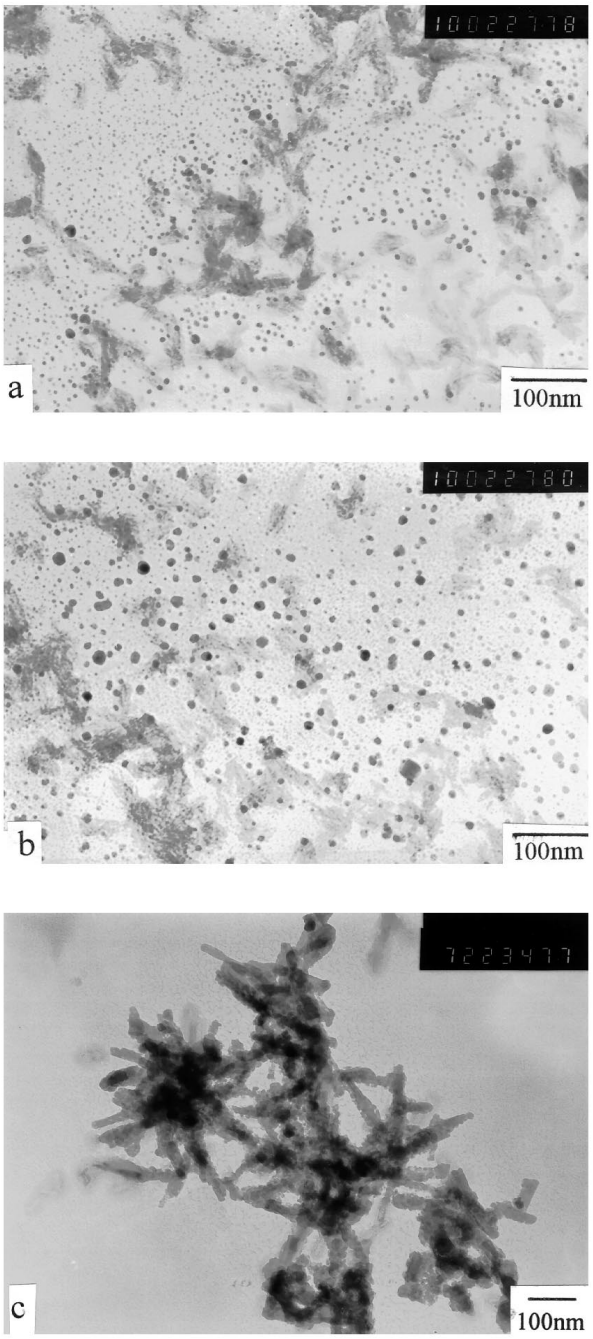

Fig. 3 TEM micrographs showing hydroxyapatite particles obtained from compositions A (a), B (b) and C (c).

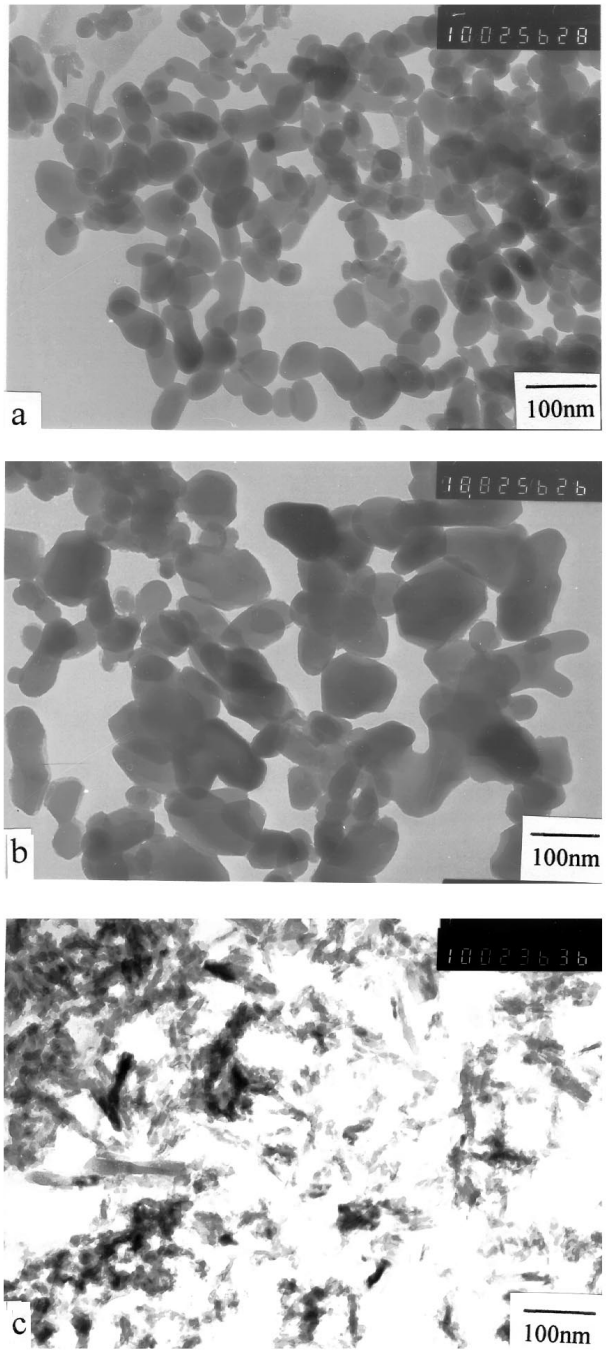

Fig. 4 TEM micrographs showing hydroxyapatite particles obtained from compositions A (a), B (b) and C (c), after calcination at 650 °C for 6 h.

The XRD patterns for the calcined hydroxyapatite powders obtained from compositions A, B and C, before and after calcination, are shown in Fig. 5(a,b), respectively. Due to the ultrafine nature of the as-precipitated crystallites, there is an extensive degree of peak broadening in the X-ray diffraction patterns for all the three powders before calcination. In comparison however, the powder from the oil-in-water emulsion exhibits a higher crystallinity, as indicated by the splitting of the broadened peaks over the 2θ region 30–35°. This is supported by the TEM micrographs shown in Fig. 3(a–c) where a larger crystallite size is observed in (c) than those in (a) and (b). When calcined at 650 °C for 6 h, the two powders from the inverse microemulsion (composition A) and inverse emulsion (composition B) underwent a considerable degree of particle and crystallite coarsening. This is demonstrated by the greater sharpness of the diffraction peaks obtained after calcination compared to those obtained before. As shown in Fig. 5(b), the splitting of the 31.8, 32.2 and 32.8° peaks took place over the 2θ range of 31–33° due to the increased degree of crystallinity. In contrast, the powder obtained from the oil-in-water emulsion (composition C) exhibits a notably higher degree of peak broadening than the other two, which is consistent with what was observed using TEM, as shown in Fig. 4(a–c) for the calcined HA powders. The occurrence of other calcium phosphate phases was not observed for any of the three hydroxyapatite powders.

Fig. 6 shows the FTIR spectra for the three HA powders obtained from compositions A, B and C, after calcination at 650 °C. The characteristic bands for hydroxyapatite appear in the regions 900–1200 cm^{-1} for phosphate stretching, and 500–600 cm^{-1} for phosphate bending. The two bands at 631 and 3571 cm^{-1} may be regarded as an indication of the crystallinity of hydroxyapatite. All these characteristic bands

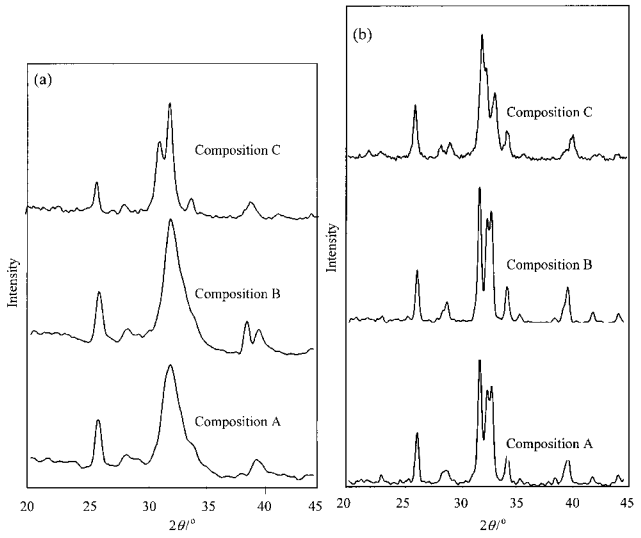

Fig. 5 XRD traces of hydroxyaptite powders obtained from inverse microemulsion, inverse emulsion and emulsion before (a) and after (b) calcination at 650 °C for 6 h.

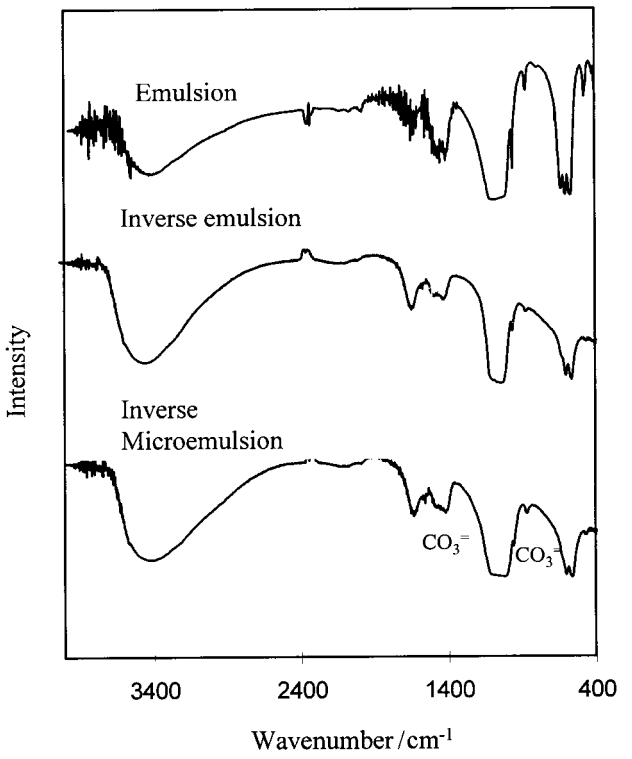

Fig. 6 FTIR spectra for the hydroxyapatite powders obtained from inverse microemulsion and emulsions, upon calcination at 650 °C for 6 h.

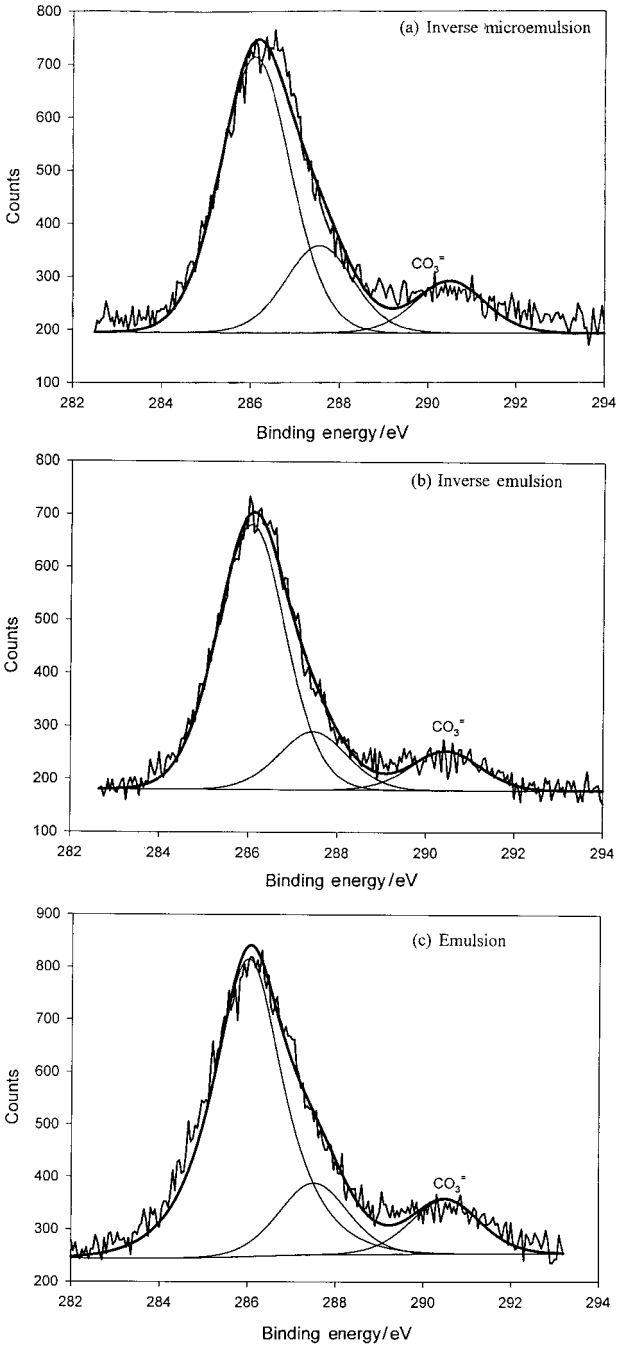

Fig. 7 XPS spectra in the C 1s region for the hydroxyapatite powders obtained from inverse microemulsion (a), inverse emulsion (b) and emulsion (c), after calcination at 650 °C for 6 h.

are observed in the spectra of the three powders. There are three additional transmission bands at 1470, 1414 and 872 cm^{-1} in all three spectra, which are attributed to carbonates that have substituted certain phosphate positions in the lattice of hydroxyapatite.[15,16] Such substitution is termed as type B substitution, in contrast to the type A subsitution where carbonates replace the hydroxyl groups. This reveals that a certain level of carbonate substitution has taken place in the three hydroxyapatite powders, although this is not shown by the XRD phase analysis.

Fig. 7(a–c) illustrate the XPS spectra in the C 1s region for the calcined HA powders obtained from the three compositions. The first deconvoluted peak at *ca.* 286 eV is due to the aliphatic hydrocarbons adsorbed on the particle surface from the XPS vacuum chamber. The second one at *ca.* 287.6 eV is attributed to C–O adsorption on the surface of the HA particles. Carbonate substitution in all three hydroxyapatites calcined at 650 °C is shown by the presence of a peak at 290.5 eV. The occurrence of carbonate substitution in hydroxyapatite has been previously reported.[17,18] In particular, type B carbonate substitution is frequently encountered in hydroxyapatite powders prepared *via* wet-chemistry routes, while type A carbonate substitution occurs in those formed through solid state reactions.[15,19] The precipitation reactions in the microemulsion and emulsions apparently resulted in the type B substitution observed in this work.

The occurrence of carbonate substitutions in hydroxyapatite is not undesirable for many applications. In a number of biological apatites, carbonates are the principal minor constituents[18] where they substitute certain phosphate positions in the biological apatites (type B). For example, the amount of

carbonate present in enamel, dentine and bones is estimated to be around 3.5, 5.6 and 7.4 wt%, respectively.[19] Synthetically carbonated apatites have been prepared by deliberately adding sodium bicarbonate to precipitated gelatinous hydroxyapatite.[20] It is thus interesting to note that the precipitation reaction in the microemulsion and emulsions led to a level of carbonate substitution when a carbonate salt was not deliberately added. These carbonates cannot be eliminated by calcination at temperatures up to 650 °C. This is different from conventionally precipitated hydroxyapatite, which is almost carbonate free upon calcination at 650 °C, as observed by FTIR. Thus, the carbonate substitution in the inverse microemulsion and emulsion-derived hydroxyapatites is believed to originate from the organic oil and surfactant phases involved in the microemulsion and emulsion compositions, although the involvement of atmospheric carbon dioxide cannot be completely ruled out.

Conclusions

Nanosized hydroxyapatite powders have been successfully prepared in an inverse microemulsion and emulsions, consisting of 1.0 M $CaCl_2$ as the aqueous phase, PE as the oil phase and biodegradable KB6ZA as the surfactant phase. Nanoparticles of hydroxyapatite were synthesized from an inverse microemulsion and an emulsion containing 25.0 and 35.0 wt% aqueous phase, respectively. They underwent a considerable degree of particle coarsening when calcined at 650 °C for 6 h, although they were well dispersed and spherical in morphology in the as-synthesized forms. Average particle sizes of 43 and 140 nm were measured for the powders obtained from the inverse microemulsion and the emulsion, containing 25.0 and 35.0 wt% aqueous phase, respectively, as calculated on the basis of BET surface area. The oil-in-water emulsion containing 90.0 wt% aqueous phase, yielded a nanocrystalline hydroxyapatite which has a dendritic agglomerate morphology. It underwent little particle and crystal coarsening when calcined at 650 °C and exhibited an average particle size of 25 nm after calcination at 650 °C for 6 h. The inverse microemulsion- and emulsion-derived hydroxyapatites exhibit a degree of type B carbonate substitution, which cannot be eliminated by calcination in air at 650 °C.

References

1 K. de Groot, *Bioceramics of Calcium Phosphate*, CRC Press, Boca Raton, FL, 1984.
2 K. de Groot, *Biomaterials*, 1980, **1**, 47.
3 L. L. Hench, *J. Am. Ceram. Soc.*, 1991, **74**, 1487.
4 P. Ducheyne, L. L. Hench, A. Kagan, M. Martens, A. Burssen and J. Muller, *J. Biomed. Mater. Res.*, 1980, **14**, 225.
5 T. Takaoka, M. Okumura, H. Ohgushi, K. Inone, Y. Takakura and S. Tamai, *Biomaterials*, 1996, **17**, 1499.
6 T. Suzuki, T. Hatsushika and Y. Hayakawa, *J. Chem. Soc., Faraday Trans. 1*, 1982, **78**, 3605.
7 J. Reichert and J. G. P. Binner, *J. Mater. Sci.*, 1996, **31**, 1231.
8 T. Kanazawa, *Materials Science Monographs: Inorganic Phosphate Materials*, Elsevier, Tokyo, 1989, pp. 15–76.
9 G. K. Lim, J. Wang, S. C. Ng and L. M. Gan, *Mater. Lett.*, 1996, **28**, 431.
10 G. K. Lim, J. Wang, S. C. Ng, C. H. Chew and L. M. Gan, *Biomaterials*, 1997, **18**, 1433.
11 M. R. Porter, *Handbook of Surfactants*, Chapman and Hall, New York, 1991.
12 R. D. Swisher, *Surfactant Biodegradation*, Marcel Dekker Inc., New York, 1970.
13 J. Sanchez Leal, M. T. Garcia, I. Ribosa and F. Cornelles, in *Surfactant in Solutions*, ed. K. L. Mittal, *Surfactant Science Series Vol. 64*, Marcel Dekker, New York, 1996, p. 379.
14 J. H. Clint, *Surfactant Aggregation*, Chapman and Hall, New York, 1992.
15 J. C. Elliot, *The Crystallographic Structure of Dental Enamel and Related Apatites*, PhD Thesis, University of London, 1964.
16 W. H. Emerson and E. E. Fisher, *Arch. Oral Biol.*, 1962, **7**, 671.
17 R. Z. LeGeros, *J. Dent. Res.*, 1990, **69**, 567.
18 R. Z. LeGeros, *Biological and Synthetic Apatites* in *Hydroxyapatite and Related Materials*, ed. P. W. Brown and B. Constantz, CRC Press, Boca Raton, FL, 1994.
19 R. Z. LeGeros, *Prog. Cryst. Growth Charact.*, 1981, **4**, 1.
20 L. G. Ellies, D. G. A. Nelson and J. D. B. Featherson, *J. Biomed. Mater. Res.*, 1988, **22**, 541.

Paper 8/09644I